2016 Caltech Report to SCEC

SCEC Award: 16050

SCEC Community Data Products of Relocated Seismicity and Improved Focal Mechanisms for Resolving Fine-Scale Fault Structures and State of Stress in Southern California

Egill Hauksson
Seismological Laboratory
California Institute of Technology
Pasadena, CA 91125
hauksson@gps.caltech.edu

14 March 2017

Abstract

The latest version of our waveform-relocated catalog (the HYS catalog) contains high-precision locations of over 597,000 earthquakes from 1981 through 2016.

In 2016 we focused on analyzing how the earthquakes focal depths depend on the velocity model used. Earthquake focal depths are difficult to determine because they are strongly dependent on the availability of P and S travel time data and the velocity model. We investigate how refined velocity models could possibly improve depth determination for the refined SCN catalog. Using a velocity model obtained from the waveform tomography as starting model (Lee et al., 2014), we invert for a new model that fits the P and S travel times best. We find out that focal depths relocated with the new model or with the waveform tomography model are shallower than those relocated with a previous travel time tomography model. In addition, the relative locations cluster differently, forming fewer but larger clusters.

Results: Relocations 1981 – 2016

The relocated (1981 – 2016) HS catalog of more than 597,000 earthquakes is shown in Figure 1. The complex spatial distribution of the events reflects the different processes that contribute to the generation of both background and triggered seismicity. The Pacific North-America plate tectonic deformation is the main process that causes major earthquakes and their aftershock sequences. Secondary processes such as geothermal exploitation, extensional gravitation collapse, or crustal delamination also cause ongoing seismicity.

The overall pattern of seismicity shows familiar features including mainshock-aftershock sequences such as 1992 Landers, 1994 Northridge, 1999 Hector Mine, and 2010 El Mayor-Cucapah. Other regions such as the southern Sierra and Coso regions, the San Jacinto fault, and the Salton Trough also have high ongoing levels of seismicity.

Results: Focal Mechanism Catalog: 2015 & 2016

In 2012 we published a large refined catalog of focal mechanisms for 1981 to 2010 using the HASH method of *Hardebeck and Shearer* (2002, 2003.). We have updated this catalog for 2011, 2012, 2013, 2014, 2015, and 2016/06. We plan to keep updating this catalog based on the latest relocated hypocenters.

We have added the following recent improvements to our focal mechanism processing: 1) the capability to use the latest relocations from the refined catalog; 2) modified scripts to use already-downloaded sac waveforms; 3) corrected the code to better include known instrument reversals by referring to station by net code, station, code and location code.

Exemplary Figure (see Figure 1 in report)

SCEC Science Priorities: 2a, 2d, 2f

Intellectual Merit

This project relates to many key SCEC objectives and will improve our understanding of earthquake activity across southern California. In particular, our high-resolution earthquake locations provide better delineation of fault structures and make possible more advanced seismicity studies by us and other SCEC researchers. Our focal mechanism catalogs and stress drop analyses provide fundamental insights into the earthquake rupture process and the relationships between micro-earthquake activity, the crustal strain field, and major faults.

Broader Impacts

Outreach activities consist of providing the relocated catalog to SCEC scientists and others doing research on seismicity in southern California. The relocated catalog is available at the Southern California Earthquake Data Center (SCEDC). We have also presented results at SCEC workshops.

Project Publications

Goebel, T. H. W., S.M. Hosseini, F. Cappa, E. Hauksso, J.-P. Ampuero, F. Aminzadeh and J.B. Saleeby (2016), “Wastewater disposal and earthquake swarm activity at the southern end of the Central Valley, California”, *Geophys. Res. Letts*, 43, 1-8, doi:10.1002/2015GL066948.

Hauksson, E. and W. Yang, and P. M. Shearer (2012), Waveform Relocated Earthquake Catalog for Southern California (1981 to June 2011); *Bull. Seismol. Soc. Am.,* **102**, no. 5, 2239–2244, doi: 10.1785/0120120010.

Hauksson, E., J. Andrews, A. Plesch, J. H. Shaw, and D. R. Shelly (2016), The 2015 Earthquake Swarm Near Fillmore, California: Possible Dehydration Event Near the Bottom of the Over-Pressurized Ventura Basin, *Seismological, Res. Letters,*87 ,4 ,p807-815 , doi: 10.1785/0220160020

Hauksson, E., Z. E., Ross, M.-A. Meier, and L. M. Jones (2017), Evolution of seismicity near the southernmost terminus of the San Andreas Fault: Implications of recent earthquake clusters for earthquake risk in southern California, *Geophys. Res. Lett.,* 44, doi:10.1002/2016GL072026

Ross, Z. E., E. Hauksson, Y. Ben-Zion (2017), Abundant off-fault seismicity and orthogonal structures in the San Jacinto fault zone., *Sci. Adv.* 3, doi: e1601946

Yang, W., E. Hauksson and P. M. Shearer (2012), Computing a large refined catalog of focal mechanisms for southern California (1981–2010): Temporal stability of the style of faulting, *Bull. Seismol. Soc. Am.*, **102**, 1179–1194, doi: 10.1785/0120110311.

SCEC Report 2016

Exemplary Figure

The Pacific North-America plate tectonic deformation is the main process that causes seismicity, including major earthquakes and their aftershock sequences. In addition secondary processes, such as geothermal exploitation, extensional gravitation collapse, or crustal delamination, cause ongoing seismicity. The most prominent features on the map consists of large aftershock sequences, such as 1992 Landers, 1994 Northridge, 1999 Hector Mine, and 2010 El Mayor-Cucapah, and regions of ongoing seismicity, such as occurs along the San Jacinto Fault, as well as many localized clusters in swarm areas.

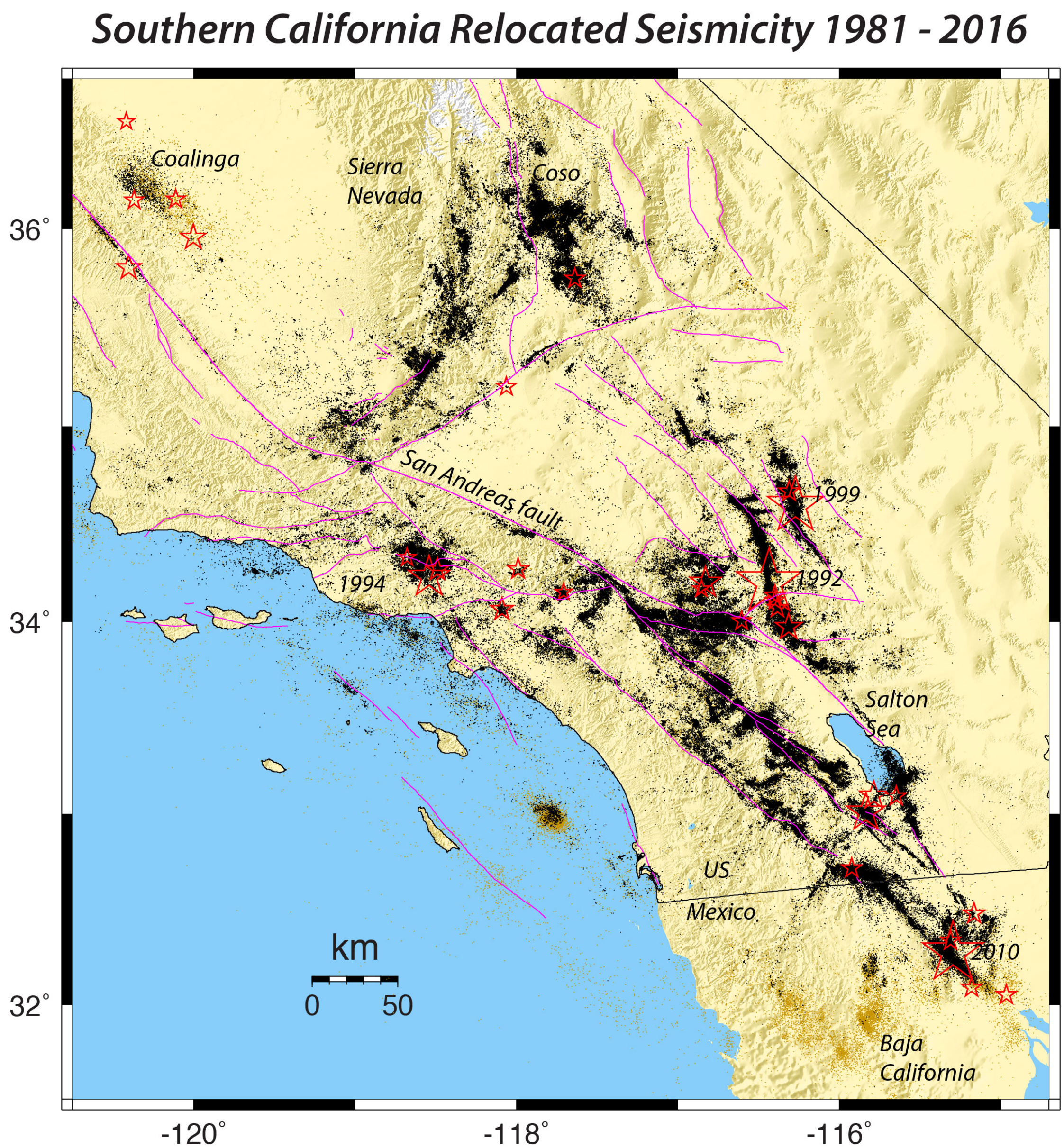

Figure 1. (Exemplary Figure) Event locations from the HYS catalog (1981 – 2016). Similar-event clusters that have been relocated by using waveform cross-correlation are shown in black. Events in the SCSN catalog (and uncorrelated events in the other catalogs) are shown in brown. Events with M ≥ 5.5 are shown as stars. Faults are from Jennings (2010) with late Quaternary faults in shades of red (Hauksson et al. 2012).

Summary

The latest version of our waveform relocated catalog (the HYS catalog) contains high-precision locations of over 597,000 earthquakes from 1981 through 2016.

In 2016 we focused on analyzing how the earthquakes focal depths depend on the velocity model used. Earthquake focal depths are difficult to determine because they are strongly dependent on the availability of P and S travel time data and the velocity model. We investigate how refined velocity models could possibly improve depth determination for the refined SCN catalog. Using a velocity model obtained from the waveform tomography as starting model (Lee et al., 2014), we invert for a new model that fits the P and S travel times best. We find out that focal depths relocated with the new model or with the waveform tomography model are shallower than those relocated with a previous travel time tomography model. In addition, the relative locations cluster differently, forming fewer but larger clusters.

Introduction

Here we compare two 3D velocity models used in southern California, the Hauksson (2000) (hereinafter referred as HKS) model obtained from travel time tomography, and the Lee et al. (2014) (hereinafter referred as Lee) model obtained from full waveform tomography.

To improve relocations for continuously updated southern California earthquakes is a long-term goal for the SCEDC. The arrival times of direct phases have been routinely used to relocate without involving additional phases. Among the four hypocenter parameters (x, y, z, t_0), the depth z is most difficult to be well constrained for several reasons. The number of high-quality S picks is usually far smaller than P picks and focal depth is mainly constrained by S-wave travel time. Also, depth has a tradeoff with origin time t_0, which can be reduced if the closest S-wave record is within 1.4 focal depth's distance (Gomberg et al., 1990). Inaccurate velocity model approximation can also bias depth determination. In this study, we focus on how different velocity models affect the depth constraint when we ensure the events have enough S picks within a close distance.

Procedures and Results

We choose a subarea with sufficient station coverage for testing. This area encompasses part of the Eastern California Shear Zone and includes the Landers-Hector Mine earthquake rupture fault segments. It is also one of the regions that host the most active clusters using the relocated catalog of Hauksson et al. (2012). The clusters can be used to assess whether the relative locations will also change after the earthquake absolute locations are improved using a new velocity model.

1. Comparison of 3D velocity models

The map views show the difference between the HKS model and the Lee model in our study area (Figure 2). Compared to the HKS model, the Lee model contains more low Vp anomalies near the surface especially at the segment of the San Andreas Fault close to the Salton Sea. In the middle crust, more fast Vp anomalies near the major faults are shown in Lee model. The velocity models are mapped with horizontal gridding at 15 km. The differential Vp value between two models in the same grid is highest at the 1 km depth with mean difference of 14% and becomes smaller for the depths of 4, 6, 10 km with mean difference of 2-3%. Below 10 km depth, the mean difference is smaller than 1%. Overall, the Lee model reveals more velocity anomalies than the HKS model.

To evaluate which model is better and closer to the "true" velocity model, we conduct two tests, one keeping starting model fixed and inverting for locations only, and the other one simultaneously inverting for locations and velocity models. The two sets of relocated locations simultaneously inverted with velocity models converge to each other while the inverted two velocity models also converge, especially at depths of 10-15 km (Figure 2). The results suggest that the two different models are being iterated close to the "true" model that also gives the "best" locations. Therefore, to obtain improved hypocenters it was necessary to construct a new velocity model that provides an improved fit for the locations.

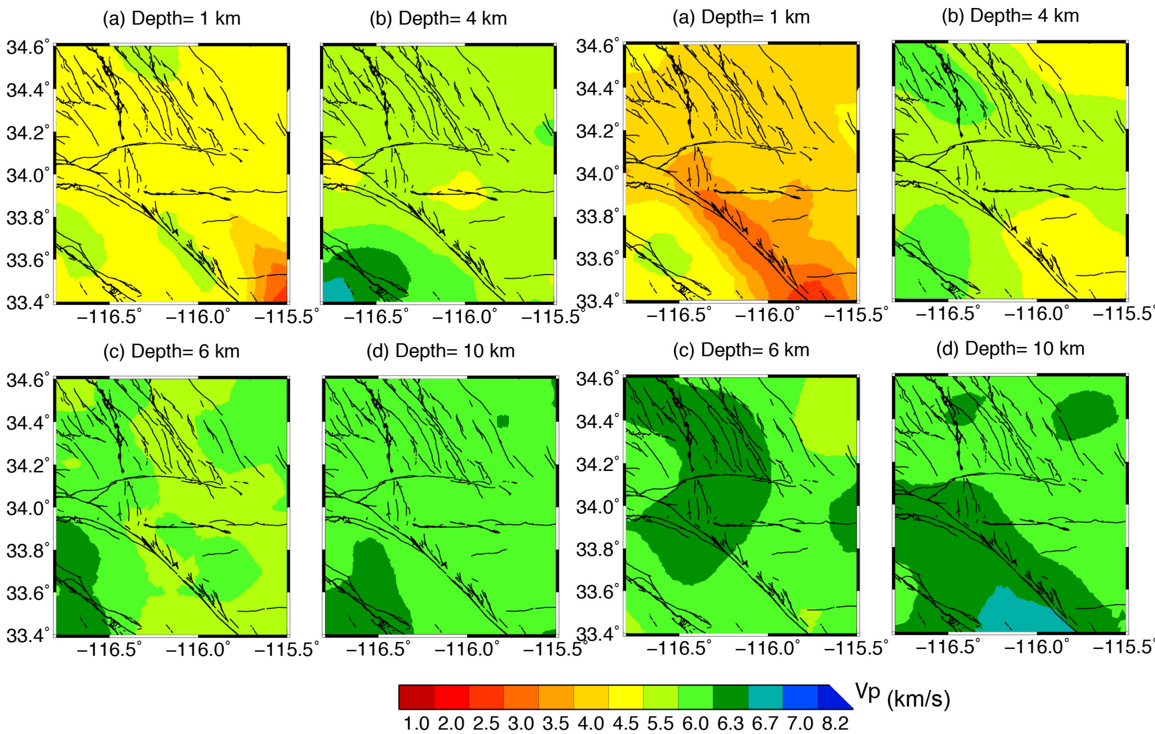

*Figure 2. Map views of the HKS model (left 4 panels) and the Lee model (right 4 panels) in our study area. The grid sizes are 15*15 km and depths slices are at depths of 1, 4, 6, 10 km.*

2. Inversion for a "better" model

One difficulty in travel time tomography is that the velocity structure cannot be well constrained near the surface because the rays are dominantly vertical in the shallow depths. Considering that the Lee model has used information from surface wave and has reasonably good resolution near the surface, we use Lee model as starting model and fix the upper 5 km depth in the inversion. To reduce computational cost and more efficiently test different sets of parameters, we choose 2565 events with > 13 P picks and > 8 S picks from the whole 72600 events for inversion. The selected events are distributed in blocks with 3*3 km in horizontal and 2 km in depth. After tuning the best parameters including damping parameter, iteration numbers, and eigenvalue cutoff, we obtain the output velocity model (hereinafter referred as Our model). Next, we fix three models (HKS, Lee, Our) and apply them to relocate locations only. Our model yields the smallest P and S residuals compared to the locations using the HKS and Lee models.

3. Comparison of absolute locations

With the three velocity models, the HKS, Lee, and Our model, we obtain three sets of relocated locations, which are referred as the HKS relocation, the Lee relocation, and our relocation. They all have improved the original SCEC locations shown by disappearing of horizontal streaks and clearer lineament in depth. They also bring SCEC earthquakes to deeper depths with a mean shift of 2 km. We compare the three sets of relocations to check if there is any systematic location shift. The difference of horizontal locations is at the level of 0.2 km, while the focal depth can vary more than 3 km. To ensure the focal depth is well constrained, we only choose events with more than 10 S picks and the closest S record is within 20 km distance, which is calculated as 1.4 times of the maximum depth (15 km). Figure 3 shows that the Lee relocation and our relocation are shallower than the HKS relocation. The map views and cross-sections reveal that a group of events at the northern end of the fault (0-20 km distance from the north) are relocated to near surface with our model or Lee model, and they have depth differences greater than 3 km compared to the HKS relocation. For this group of events, S picks are available at stations with azimuth gap less than 90°.

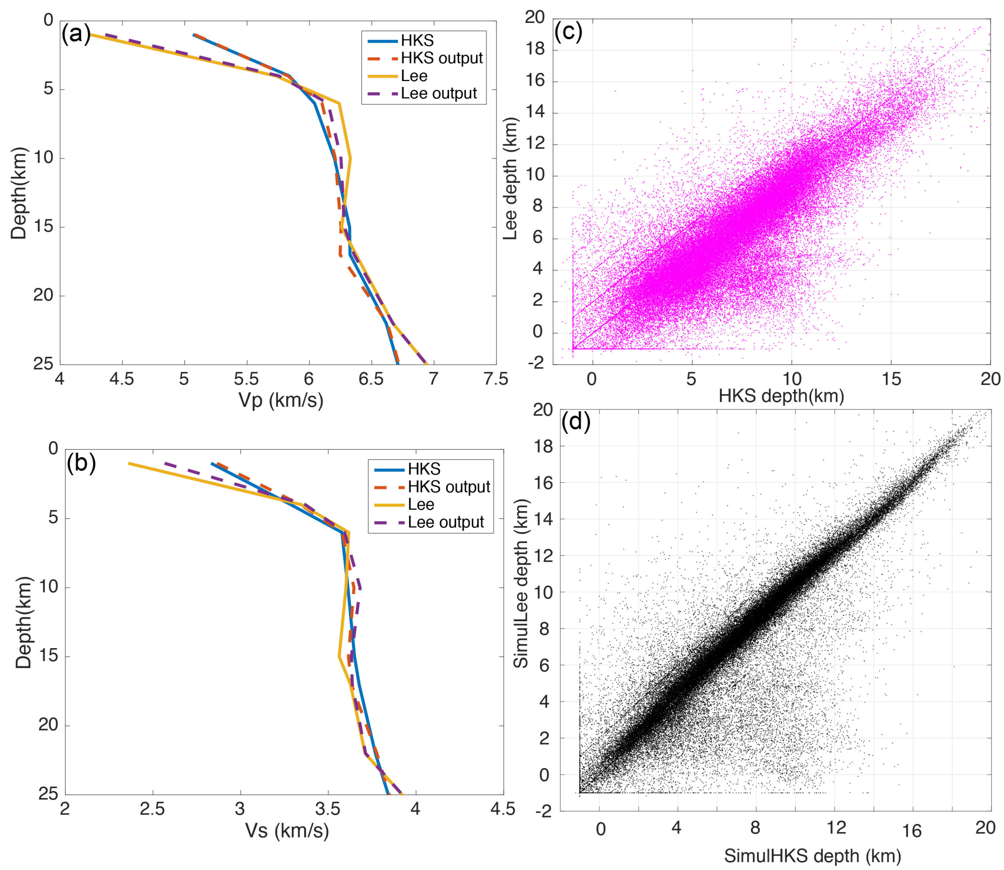

Figure 3. Results of two inversion tests. Comparison of input 1D Vp (a) and Vs (b) and output Vp and Vs models with simultaneous inversions for earthquake locations. (c) Relocated earthquakes without inversion for velocity models. (d) Relocated earthquakes with simultaneous inversion for velocity models.

4. Distribution of clusters

Because the Lee model has more velocity anomalies than the HKS model, we expect that relative locations of some earthquakes could be also affected. Following the method of Zhang and Shearer (2016), we search clusters from the three sets of locations. The algorithm considers 3D locations and occurring time and find events clustered in time and space with higher density than the background events. A total of 100 clusters can be found from the HKS relocation, while 79 clusters are found from the Lee relocations. Since the difference in horizontal locations is smaller than 1 km, the difference in clusters distributions mainly results from the depth difference. Improved depths lead to more accurate identification of clusters. As illustrated in Figure 4 cross-sections, the cluster at the distance of 0-20 km from the north in the HKS relocations has been divided to two groups in the Lee or our relocations. Note that our model has used the Lee model as starting model and still inherits some velocity similarity, thus the cluster distribution is also similar with 85 clusters identified.

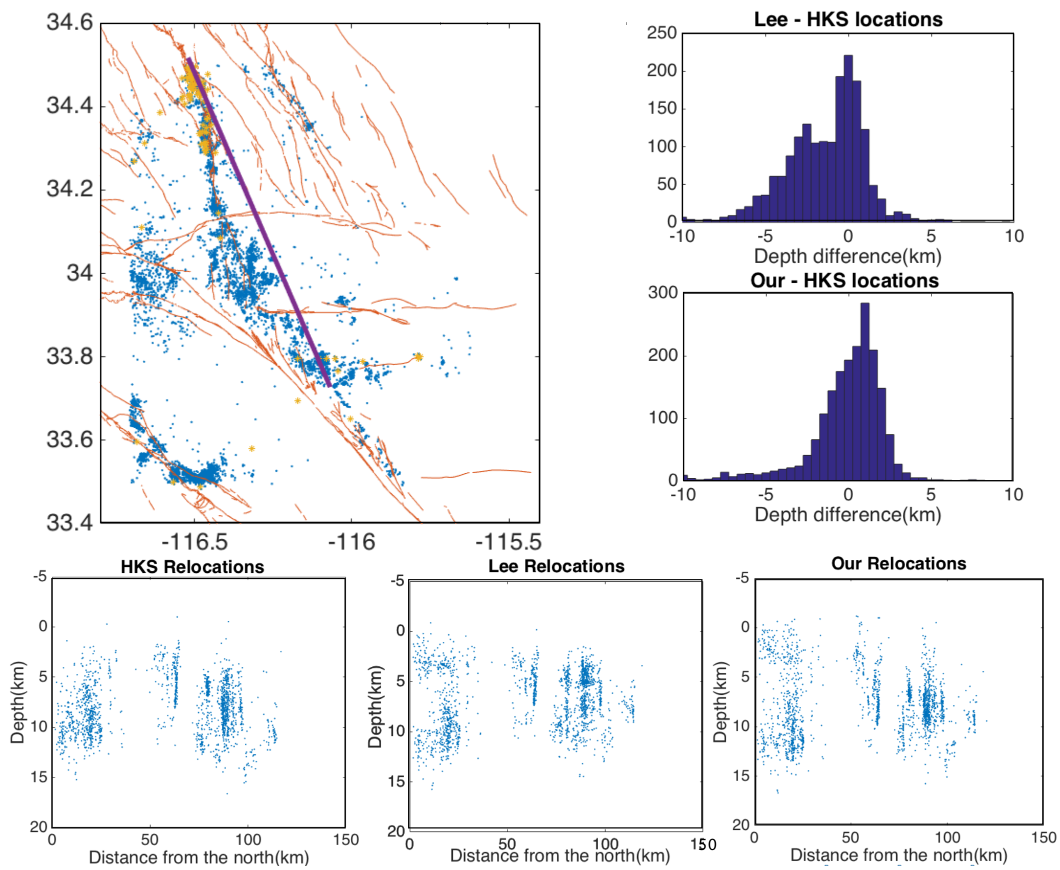

Figure 4. Map views and cross-sections comparison of three sets of relocations. On map view, the blue dots denote the earthquakes with magnitude >1, S picks >10, and the closest S record < 20 km. Yellow dots represent the events with significant depth difference greater than 5 km. Two histograms show depth comparisons of events included in the cross sections.

References

Gomberg, J. S., K. M. Shedlock, and S. W. Roecker (1990), The effect of S-wave arrival times on the accuracy of hypocenter estimation, *Bulletin of the Seismological Society of America*, *80*(6), 1605-1628.

Hauksson, E. (2000), Crustal structure and seismicitydistribution adjacent to the Pacific and North America plate boundary in southern California, *J. geophys. Res*, *105*(B6), 13875-13903.

Hauksson, E., W. Yang, and P. M. Shearer (2012), Waveform Relocated Earthquake Catalog for Southern California (1981 to June 2011), *Bulletin of the Seismological Society of America*, *102*(5), 2239-2244, doi:10.1785/0120120010.

Lee, E. J., P. Chen, T. Jordan, P. B. Maeching, M. A. M. Denolle, and G. Beroza (2014), Full-3-D Tomography for Crustal Structure in Southern California.pdf, *J. geophys. Res*, *119*(9), 6421-6451.

Zhang, Q., and P. M. Shearer (2016), A new method to identify earthquake swarms applied to seismicity near the San Jacinto Fault, California, *Geophysical Journal International*, *205*(2), 995-1005, doi:10.1093/gji/ggw073.

Hauksson, E., W. Yang, and P. Shearer, Waveform relocated earthquake catalog for southern California (1981 to June 2011), *Bull. Seismol. Soc. Am.*, 102, 2239–2244, doi: 10.1785/0120120010, 2012.

Jennings, C.W., Bryant, W.A., 2010. 2010 Fault Activity Map of California. Geologic Data Map No. 6, California Geological Survey, Sacramento CA.